ISSN 2070-2051, Protection of Metals and Physical Chemistry of Surfaces, 2016, Vol. 52, No. 5, pp. 832–838. © Pleiades Publishing, Ltd., 2016.
Original Russian Text © A.N. Kokatev, I.V. Lukiyanchuk, N.M. Yakovleva, V.S. Rudnev, E.A. Chupakhina, A.N. Yakovlev, K.V. Stepanova, 2016, published in Fizikokhimiya Poverkhnosti i Zashchita Materialov, 2016, Vol. 52, No. 5, pp. 517–524.

NANOSCALE AND NANOSTRUCTURED MATERIALS AND COATINGS

Catalytically Active Composite Materials with Porous Aluminum Oxide Matrix Modified by γ-MnO_2 Nanoparticles

A. N. Kokatev[a], I. V. Lukiyanchuk[b], N. M. Yakovleva[a, *], V. S. Rudnev[b, c, **], E. A. Chupakhina[a], A. N. Yakovlev[d], and K. V. Stepanova[a]

[a] *Petrozavodsk State University, ul. Lenina 33, Petrozavodsk, Republic of Karelia, 185910 Russia*
[b] *Institute of Chemistry, Far-Eastern Branch, Russian Academy of Sciences, pr. 100-letya Vladivostoka 159, Vladivostok, 690022 Russia*
[c] *Far Eastern Federal University, ul. Sukhanova 8, Vladivostok, 690950 Russia*
[d] *LLC Nelan-Oxide Plus, ul. Rovio 17, bldg 2, kv. 69, Petrozavodsk, Republic of Karelia, 185026 Russia*
**e-mail: nmyakov@petrsu.ru*
***e-mail: rudnevvs@ich.dvo.ru*

Received December 25, 2015

Abstract—Manganese dioxide has been deposited on the surface of an aluminum foil anodized in 3% solution of oxalic acid using the methods of thermal decomposition of manganese nitrate and potassium permanganate, as well as chemical synthesis, in the same solutions with intermediate drying and subsequent annealing. It has been demonstrated that the method of thermal decomposition of potassium permanganate is the most suitable for producing thermally stable "ultradispersed γ-MnO_2/nanostructured Al_2O_3/Al" composites. The produced composites are active in the reaction of oxidation of CO into CO_2 at temperatures above 180°C. Studies by means of the methods of scanning electron and atomic force microscopies have shown that the concentration and surface distribution of γ-MnO_2 particles depend on the morphological structure of aluminum oxide that is determined by conditions of the metal surface pretreatment and application of the pore broadening operation.

DOI: 10.1134/S2070205116050130

INTRODUCTION

At present, the unfavorable ecological situation is making it necessary to develop new efficient technologies of air decontamination, the application of which will allow improving living and working conditions. The problem of reduction of hazardous emissions into the environment can be solved, in particular, through application of catalysts. The most extensively used and efficient of which are the catalysts containing noble metals (Pt, Pd) deposited on ceramic or metallic substrates [1–3]. In many cases, to deposit catalytically active compounds on a metallic substrate, it is necessary to apply a 'sublayer' (or a secondary substrate) improving the adhesion to the metallic base and increasing the catalyst specific surface area (as compared to that of a metal). The controlled aluminum anodization resulting in formation of a nanoporous thermally and mechanically stable oxide layer characterized with regular porous structure and high adhesion to the metallic substrate on its surface constitutes a promising method of producing a secondary substrate on aluminum and its alloys with characteristics suitable for catalytic processes at temperatures up to 600°C [1, 4, 5]. Such nanoporous anodic oxide films with high specific surface area can be used as matrices for deposition of catalytically active compounds and particles, i.e., a basis for creating composite coatings with catalytic properties [6–8].

The authors of [7, 8] examined the possibility of creating catalytically active oxide systems through modification of porous anodic aluminum oxide by noble metal particles. Recently, the interest of researchers has shifted to composites based on transition metal oxides, the activity of which is often not inferior to that of catalysts made of noble metals, while their cost is much lower [9, 10]. Here, manganese dioxide—one of the most active catalysts of CO, C_xH_y, and NO_x oxidation—can serve as an example [11–14].

Thermal or hydrothermal (in the presence of water vapor) decomposition of manganese salts (pyrolysis) is applied to deposit manganese oxides on a solid surface, including that of oxide layers [11, 15]. As a rule, pyrolysis on the surface of anodic aluminum oxide at temperatures in the range of 200–350°C results in the formation of the polycrystalline manganese oxide of a complex phase composition comprising a combina-

tion of poorly ordered β-MnO_2 and finely crystalline γ-MnO_2 [11] phases. At the pyrolysis temperature increase above 450°C, lower-valence oxides (Mn_2O_3, Mn_3O_4, and, possibly, MnO) appear in the composition of reaction products.

Also, the electrochemical synthesis consisting in the electrolysis of solutions containing manganese salts is used to obtain manganese oxides [11, 16]. Usually, a solution of manganese sulfate with additions of sulfuric acid and dopants (in particular, salts of alkali metals, for example, lithium sulfate) is used. Dopants allow variations of the dispersity and sorption activity of the obtained substance [11]. Most often, both electrochemical and chemical syntheses yield the formation of the finely dispersed phase of γ-MnO_2.

Recently, techniques for producing nanosized "mesoporous" particles of manganese oxides have been suggested [13, 17, 18]. Mesoporous or ultradispersed manganese dioxides (γ-MnO_2 [17] and β-MnO_2 [18]), especially in combination with other transition metals, are active catalysts of oxidation of various volatile organic compounds, which is facilitated by their high specific surface area [19]. Mixed-valence ultradispersed manganese oxides can be formed using different methods, for example, through deposition in solutions containing MnO_4^- and Mn^{2+} ions or by the template sol–gel method [19, 20]. The values of specific surface area of the mesoporous manganese oxide could attain 200–1000 m^2/g, while the pore sizes were 1.5–3.0 nm.

In view of the above, application of "ultradispersed γ-MnO_2/nanostructured Al_2O_3/Al" composites appears to be promising in the development of catalytic systems.

The objectives of the present work consisted in selection of the method of deposition of ultradispersed MnO_2 on the surface of the nanostructured anodic aluminum oxide and estimation of the catalytic activity of the produced composites in the reaction of oxidation of CO into CO_2.

MATERIALS AND METHODS

Samples of a size of 2.5 × 2.5 cm were made of aluminum foil of two types: foil of A99 alloy of a thickness of 500 μm (hereinafter, foil-1) and anodic condenser foil of a thickness of 50 μm (hereinafter, foil-2) with a surface area 10–15 larger than the visible one.

Prior to anodization, samples of foil-1 were cleaned in 3% solution of NaOH at 40–50°C for 30 s and washed with distilled water. Samples of foil-2 were washed with ethanol and, thereafter, with distilled water. Upon washing, both types of samples were dried in air at room temperature. Prior to anodization, the samples that were further used in catalytic activity tests were rolled up into tubes of a diameter of 7–8 mm.

Anodization was carried out in 3% aqueous solution of oxalic acid ($C_2H_2O_4$) at constant current density j_a (galvanostatic mode (GSM)) and a temperature of 8°C using a two-electrode cell with a lead cathode. Samples of foil-1 were anodized at $j_a = 10$ mA/cm^2 for $t = 1$ h. The thickness of anodic oxide films (AOFs) formed under above conditions on the surface of foil was δ ~ 15 μm. Anodization of a thinner foil-2 was carried out under conditions excluding the electrolyte heating and local foil destruction: $j_a \cong 15$ mA/cm^2, $t =$ 20 min, and δ ~ 5 μm.

Upon anodization, pore broadening was performed: anodized samples were immersed for 10–15 min into 1% solution of H_3PO_4 at $T = 35$°C with subsequent washing and drying. This procedure results in the removal of the anion-containing oxide layer on pore walls and a thin upper "defect" layer of AOF [6].

To deposit ultradispersed manganese dioxide on the surface of anodic aluminum oxide, the reactions below were used: interaction between manganese nitrate and potassium permanganate

$$3Mn(NO_3)_2 + 2KMnO_4 + 2H_2O \rightarrow \rightarrow 5MnO_2 + 2KNO_3 + 4HNO_3, \quad (1)$$

and thermal decomposition of potassium permanganate and manganese nitrate:

$$2KMnO_4 \rightarrow MnO_2 + K_2MnO_4 + O_2, \quad (2)$$

$$Mn(NO_3)_2 \rightarrow MnO_2 + 2NO_2\uparrow. \quad (3)$$

In the first case, the anodized sample was alternately impregnated in 5% solution of $Mn(NO_3)_2$ and then in 5% solution of $KMnO_4$ with an intermediate drying at T ~ 70°C. The process was repeated three times to produce a sufficient amount of the substance. Thereafter, the unreacted substances were washed with water and the sample was dried in air at $T =$ 150°C for 15 min.

In the second case, the anodized sample was impregnated in warm ($T = 40$°C) 5% $KMnO_4$ solution for 5 min. Then, the samples were heated in air up to T ~ 220–230°C and held at this temperature for 10 min. The water-soluble potassium manganate (K_2MnO_4) formed in reaction (2) was removed by washing in water, and the sample was dried. An increase of the manganese dioxide quantity in pores and on the surface of aluminum oxide was achieved in the cycled process (three cycles).

In the third case, the anodized samples were impregnated in 10% solution of manganese nitrate ($Mn(NO_3)_2$) and annealed in air at $T \cong 200$–230°C for $t = 5$ min. Three pyrolysis cycles were performed.

To study the structure and morphology of the sample surface, the following methods were used: scanning electron microscopy (JEOL JSM-6480LV, Japan), atomic force microscopy (SPM Solver Next, Russia), and X-ray diffraction analysis (DRON 4-07,

Russia). The features of the experimental technique and the data treatment are described in [21–23].

Catalytic tests of the produced composite structures in the model reaction of oxidation of CO into CO_2 were carried out using a *BI-CATflow4.2*(*A*) universal flow-type installation (made in Boreskov Institute of Catalysis of SB RAS). To evaluate the catalytic activity, the rolled up samples were placed into the active zone (of a diameter of 0.9 cm and a height of 3 cm) of a tubular quartz reactor. The initial reaction mixture contained 5% CO and air. The gas flow rate was 50 mL/min. The output concentrations of CO and CO_2 were determined using a PEM-2 IR gas analyzer (Russia). The studied temperature range was 20–500°C. As a rule, two cycles of catalytic tests were performed. The CO conversion was calculated according to the formula $X = \frac{C_{\text{init}} - C}{C_{\text{init}}} \times 100\%$, where C_{init} and C were the initial and final CO concentrations, respectively.

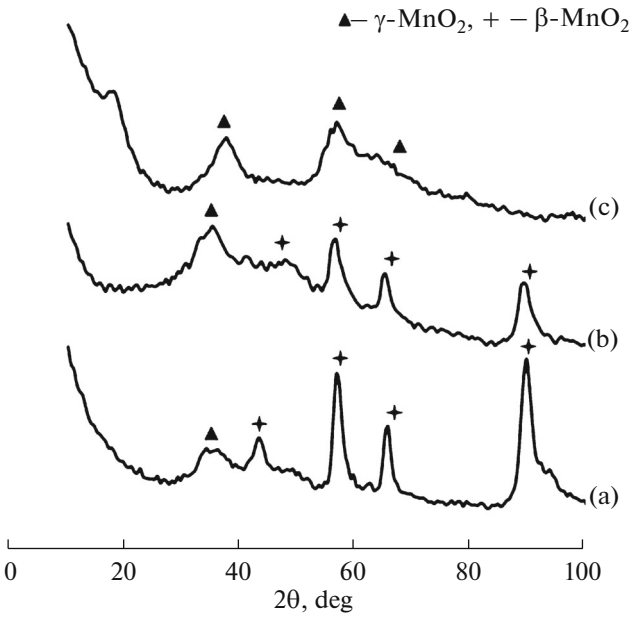

Fig. 1. X-ray diffraction patterns of aluminum samples with coatings of aluminum oxide modified with manganese dioxide as a result of (a) thermal decomposition of manganese nitrate, (b) chemical synthesis, and (c) thermal decomposition of potassium permanganate.

RESULTS AND DISCUSSION

At the first stage, the morphology and phase composition of manganese oxides deposited on anodized foil by different methods were studied. The main task consisted in selection of the method that allows fabrication of ultradispersed particles of manganese dioxide on the anodic layer surface. The X-ray diffraction analysis of the obtained manganese oxides was performed upon their mechanical separation from the anodized substrate. Note that the aluminum foil anodized in 3% solution of $C_2H_2O_4$ is easily wetted by solutions used in obtaining manganese oxides.

X-ray diffraction and microscopy studies of manganese oxides samples obtained by low-temperature pyrolysis (Eq. (3), Figs. 1a, 2a) and chemical synthesis (Eq. (1), Figs. 1b, 2b) demonstrated that, in both cases, the formation of a multiphase coating containing both low-temperature finely dispersed (γ-MnO_2) and poorly ordered (β-MnO_2) phases took place. Traces of three-valence manganese oxide (Mn_2O_3) were registered in some cases during the pyrolytic decomposition. As seen from SEM images of the chemically synthesized layer (Fig. 2b), all the surface of the anodized sample is coated by particles of various sizes. The sizes of manganese dioxide particles are in the range from 60 to 500 nm. Note that the subsequent temperature increase up to $T \geqslant 400$°C induces transformation of β-MnO_2 into Mn_2O_3.

Thus, manganese oxides produced under the used conditions of low-temperature pyrolysis of manganese nitrate (Eq. (3)) and chemical synthesis (Eq. (1)) are not characterized with the necessary thermal stability and fine dispersity.

The control of the phase composition of manganese oxides obtained using the thermal decomposition of potassium permanganate (Eq. (2)) showed the compliance of the obtained oxide with the ultradispersed γ-modification of MnO_2 (Fig. 1c). The diffused peaks on the X-ray pattern indicate the X-ray amorphous properties of the obtained substance. As was found by SEM studies, application of the above method resulted in the formation of γ-MnO_2 particles of a size from 10 to 100 nm (Fig. 2c). As seen in the image, large particles consist, in their turn, of smaller ones of a size of 5–10 nm, which is in good correlation with the diffused character of peaks shown in Fig. 1c.

To evaluate the thermal stability, the samples of manganese dioxide produced through thermal decomposition of $KMnO_4$ underwent annealing at T = 350 and 400°C. No changes were observed in X-ray diffraction patterns of the annealed samples: diffused peaks, the positions of which corresponded to the γ-MnO_2 modification, were still present.

Thus, the application of the technology of thermal decomposition of potassium permanganate at T = 220–230°C enables one to deposit thermally stable ultradispersed γ-MnO_2 nanoparticles of linear sizes in the range from 10 up to 100 nm on the AOF surface. That is why this very method was selected for modification of the anodized samples.

At the next stage, the morphology of the surface of samples of anodized foil-1 and foil-2 before and after deposition of manganese dioxide using the method of

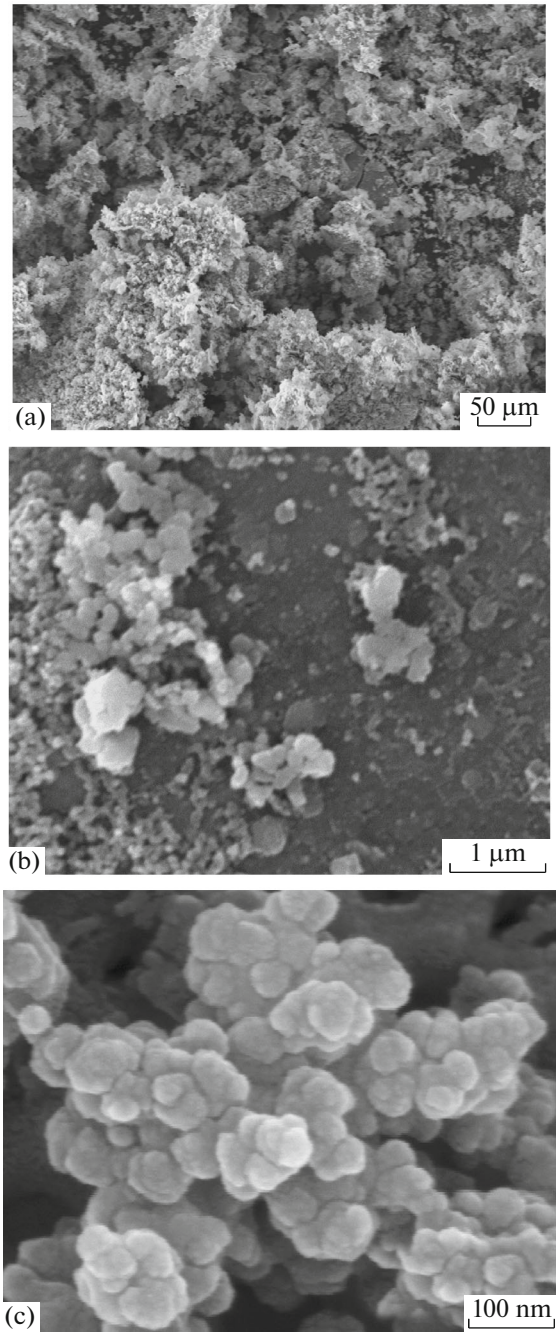

Fig. 2. SEM images of the surface of anodic oxide coatings on aluminum samples upon modification by manganese dioxide as a result of: (a) thermal decomposition of manganese nitrate, (b) chemical synthesis, (c) thermal decomposition of potassium permanganate.

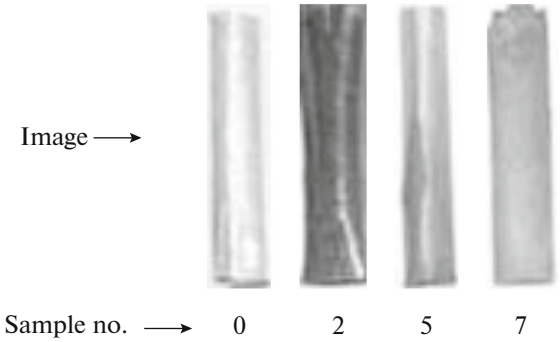

Fig. 3. Images of typical samples of foil-1 (sample 0 , after anodization; sample 2, after anodization and manganese dioxide deposition) and foil-2 (samples 5 and 7, after anodization and manganese dioxide deposition). Sample formation conditions are shown in the table.

thermal decomposition of $KMnO_4$ (Eq. (2)) was investigated. After deposition of manganese dioxide (under the same conditions; see table) on the anodized foil, the samples colors changed: samples of the foil-1 acquired a homogeneous dark (close to black) color, whereas, on the surface of samples of foil-2, one observed parts that were more similar to the color of the initial anodized sample (Fig. 3).

According to the SEM data (Fig. 4), the surface of the chemically etched aluminum foil-2 is extremely heterogeneous: intensively etched parts (Fig. 4a) are present, along with sufficiently smooth ones at about equal ratio. One can see that, if anodization of the foil-2 in 3% $C_2H_2O_4$ does not add new details to SEM images (Figs. 4b, 4c), the manganese oxide deposition yields significant changes in the relief of the surface of etched parts (Fig. 4d), which must be caused by the emergence of γ-MnO_2 crystallites. Their sizes do not exceed 250 nm. At the same time, the character of the relief of smooth parts remains virtually unchanged. To sum up, analysis of the surface morphology of foil-2 samples after the stage of formation of a porous AOF with subsequent deposition of manganese oxide through thermal decomposition of potassium permanganate allows the conclusion to be drawn that there is a predominant presence of manganese dioxide on etched surface parts.

The data on the morphological surface structure in the nanosize scale were obtained using the semicontact AFM technique. The results of AFM studies showed (Fig. 5a) the presence of a so-called “defect” or “disordered” porous layer on the surface of a porous AOF formed by anodization of foil-1 and treated in 1% solution of H_3PO_4. This layer morphology reflects the state of the surface of the barrier AOF layer at the stage of pore nucleation on an unpolished metal [5, 6]. Such a structural feature of AOF is typical for the single-stage galvanostatic anodization of aluminum [5]. As a rule, the thickness of this layer is close to that of the barrier AOF layer; i.e., its value is ~100 nm under the aforementioned anodization conditions, for which reason the used conditions of pore broadening did not result in the removal of the defect oxide layer. Thus, a “defect porous layer” characterized by the presence of pore openings located in a disordered way of a size of

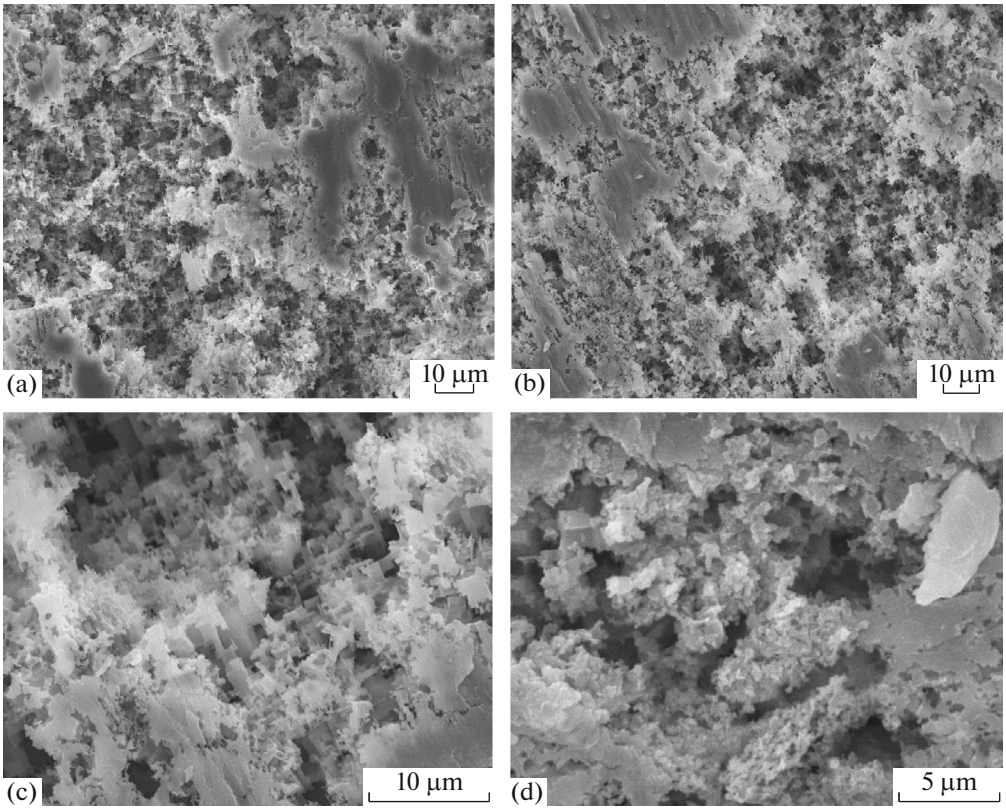

Fig. 4. SEM images of the surface of foil-2 (etched aluminum foil) (a) before and (b, c) after anodization in 3% $H_2C_2O_4$, as well as after deposition of manganese oxide, using the method of thermal decomposition of $KMnO_4$ (d).

30–50 nm, as well as numerous defects and heterogeneities, were found on the surface of AOF formed by traditional anodization on foil-1.

Upon the modification by manganese oxide, numerous round-shaped particles of linear sizes from 20 to 80 nm with predomination of the finer fraction appear in pores and defects of the surface layer. No accumulations of γ-MnO_2 nanoparticles completely shielding the AOF surface were detected. Analysis of small scanning areas with $S = 1$ μm^2 (Fig. 5b) enabled us to establish that the sample surface was coated with manganese dioxide nanoparticles of a diameter of 10–30 nm that were partially linked into larger agglomerates of a size of 50–80 nm, which is in good agreement with the SEM results (Fig. 2c). Note that a fine (up to 30 nm) fraction of manganese oxide nanoparticles is present in AOF pores with diameters of up to 80 nm.

Thus, one can conclude that, under the used experimental conditions, the thermal decomposition of potassium permanganate results in formation of γ-MnO_2 nanoparticles homogeneously distributed both over the surface and in open pores of AOF formed on foil-1.

During the AFM studies of the relief of the surface of samples formed on foil-2, parts with a rather smooth surface were selected (see Figs. 4b, 4c). It was

Characteristics of samples for AFM and catalytic activity studies

Sample no.	Metal	Anodization conditions	γ-MnO_2 deposition conditions
0	Foil-1	3% $C_2H_2O_4$, $T \cong 8$°C, $j_a = 10$ mA/cm^2, 1 h, pore broadening, δ ~ 15 μm	–
2			Thermal decomposition of potassium permanganate: 5% solution of $KMnO_4$, 5 min, 220–230°C, 3 cycles
5	Foil-2	3% $C_2H_2O_4$, $T \cong 8$°C, $j_a \cong 15$ mA/cm^2, 20 min, pore broadening, δ ~ 5 μm	
7			

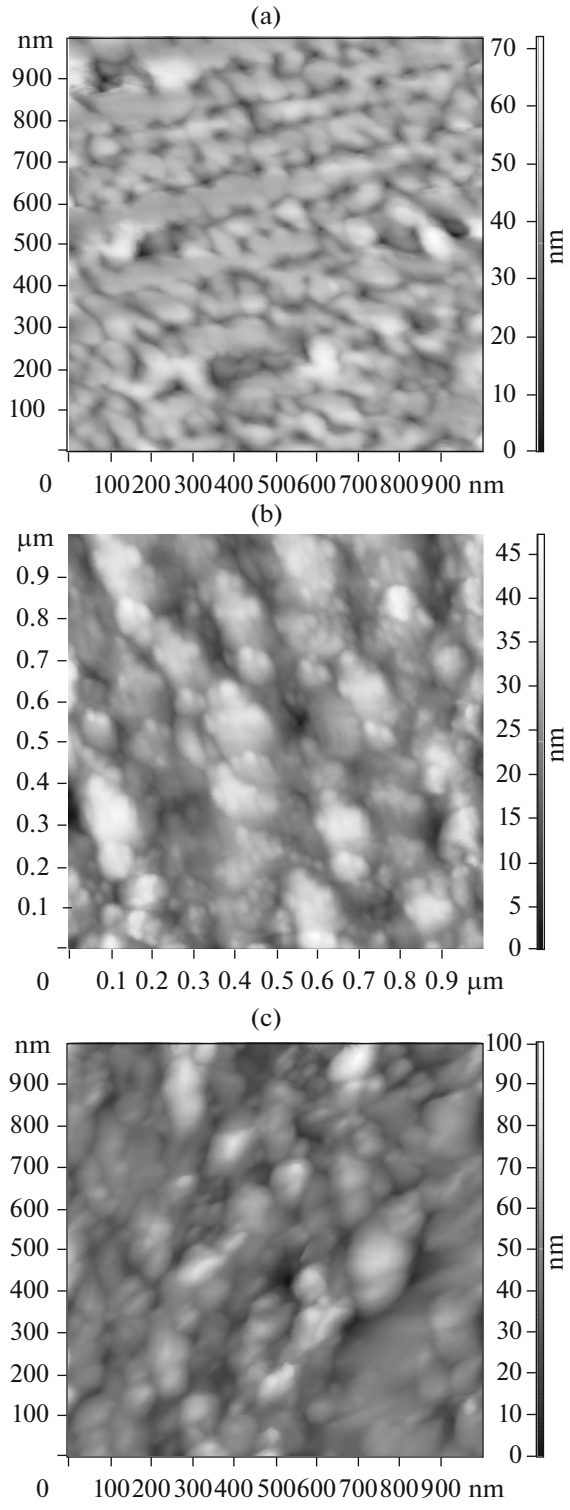

Fig. 5. AFM images of (a, b) the surface of the anodized foil-1 (a) before and (b) after deposition of manganese oxide using the method of thermal decomposition of $KMnO_4$; (c) the surface of the anodized foil-2 after deposition of manganese oxide using the method of thermal decomposition of $KMnO_4$.

found that, even in such areas, the surface was rather developed with height differences more than 1 μm. Upon anodization, the defect oxide layer with disorderly located pores of a size of 20–80 nm is present on the surface of the foil-2, which is also characteristic of the anodized foil-1. Upon modification by manganese oxide (Fig. 5c), one observes round-shaped γ-MnO_2 particles of a size of 20–100 nm on the AOF surface, which is in good agreement with the data on the size of manganese dioxide nanoparticles obtained on foil-1 (Fig. 5b). However, the density of γ-MnO_2 particles on the surface of the studied parts of samples of foil-2 is noticeably lower than that for foil-1. Thus, both SEM and AFM studies indicate that there is a heterogeneous distribution of γ-MnO_2 particles on the surface of anodized samples of foil-2: the majority of particles are concentrated in etched areas, whereas relatively smooth parts contain smaller quantities of them. Such a distribution of γ-MnO_2 particles must also determine the heterogeneous coloring of samples of foil-2, as compared to those of foil-1 (Fig. 3).

Oxidation of carbon monoxide is known [12, 24] to be accompanied with a substantial reduction of the Gibbs energy ($\Delta G^0_{298} = -242$ kJ/mol); however, the CO_2 formation without a catalyst does not occur at temperatures below 650°C. The results of catalytic tests in the reaction of oxidation of CO into CO_2 are shown in Fig. 6. As seen from the dependence of the CO conversion on temperature, the anodized samples of foil-1 manifest low catalytic activity, with the degree of transformation at 500°C not exceeding 30% (sample 0 in Fig. 6). Modification of the surface of the anodized samples of foil-1 and foil-2 by γ-MnO_2 nanoparticles results in a significant increase of the catalytic activity in the reaction CO oxidation: the temperature of the reaction start (T_{10}) is 180–240°C, whereas half-conversion temperature T_{50} = 300–350°C. For the samples of foil-2 (samples 5, 7), the degree of transformation attains 100% at a temperature about 400°C, while for those of foil-1 (sample 2) reach it at 500°C.

To sum up, it has been demonstrated that application of the reaction of thermal decomposition of potassium permanganate under the suggested conditions (see table) enables one to obtain thermally stable ultradispersed γ-MnO_2 on the surface of the nanoporous anodic aluminum oxide. The samples modified with manganese dioxide catalyze the reaction of oxidation of CO into CO_2 at temperatures above 180°C. The concentration and surface distribution of γ-MnO_2 particles depend on the morphological structure of the anodic aluminum oxide determined by the conditions of metal surface pretreatment and pore broadening application.

The produced "ultradispersed γ-MnO_2/nanostructured Al_2O_3/Al" catalytic systems may prove efficient for the removal of carbon monoxide and other

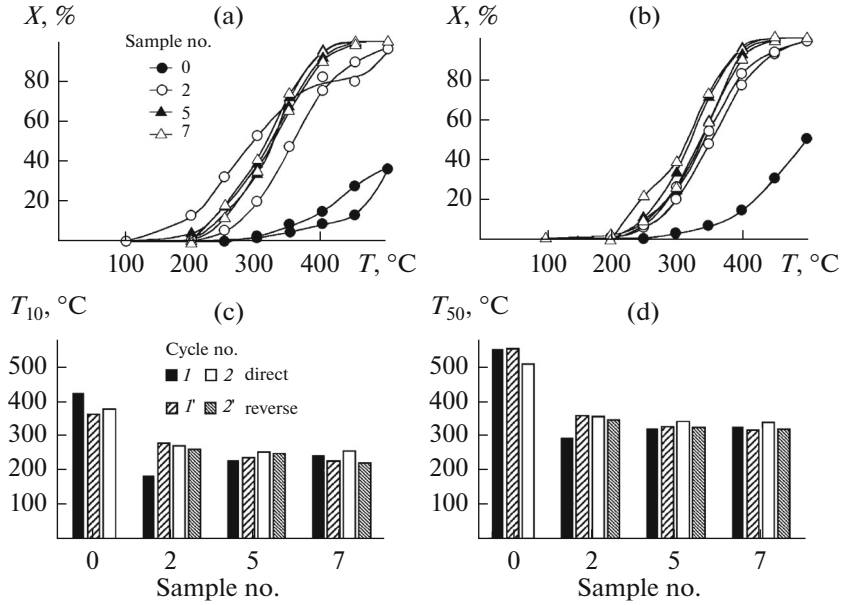

Fig. 6. Temperature dependences of CO conversion (X, %) during the (a) first and (b) second cycles of catalytic tests; temperatures of (c) conversion start (T_{10}) and (d) half-conversion (T_{50}) for the samples of the anodized foil-1 (0) and the anodized foil-1 (2) and foil-2 (5, 7) modified with manganese dioxide. The conditions of samples production are shown in the table; images of samples are in Fig. 3.

gases hazardous for human health from the air due to a combination of high specific surface area of the self-organized oxide matrix and catalytic activity of manganese dioxide nanoparticles.

REFERENCES

1. Burgos, N., Paulis, M., and Montes, M., *J. Mater. Chem.,* 2003, vol. 13, p. 1458.
2. Kondrikov, N.B., Rudnev, V.S., Vasil'eva, M.S., et al., *Khim. Interesakh Ustoich. Razvit.,* 2005, vol. 13, p. 851.
3. Rudnev, V.S., Kondrikov, N.B., Tyrina, L.M., et al., *Ser. Kritich. Tekhnol. Membrany,* 2005, vol. 28, no. 4, p.63.
4. Yakovleva, N.M., Yakovlev, A.N., and Chupakhina, E.A., *Kondens. Sredy Mezhfaznye Granitsy,* 2006, vol. 8, no. 1, p. 69.
5. Yakovleva, N.M., Kokatev, A.N., Chupakhina, E.A., et al., *Kondens. Sredy Mezhfaznye Granitsy,* 2015, vol. 17, no. 2, p. 137.
6. Kokatev, A.N., *Cand. Sci. (Eng.) Dissertation,* Moscow, 2013.
7. Burgos, N., Paulis, M., Antxustegi, M., et al., *Appl. Catal. B-Environ.*, 2002, vol. 38, no. 4, p. 251.
8. Sanz, O., Martinez, L.M., Dominguez, M.I., et al., *Chem. Eng. J.,* 2009, vol. 151, p. 324.
9. Bulachenko, O.A., Afonasenko, T.N., and Tsyrul'nikov, P.G., *Appl. Catal. A-Gen.,* 2013, vol. 459, p. 73.
10. Njagi, E.C., Chen, C.H., Genuino, H., et al., *Appl. Catal. B-Environ.,* 2010, vol. 99, p. 103.
11. Rode, E.Ya., *Kislorodnye soedineniya margantsa. Iskusstvennye soedineniya, mineraly i rudy* (Oxygen Compounds of Manganese. Artificial Compounds, Minerals and Ores), Moscow: USSR Acad. Sci., 1952.
12. Ivanova, N.D., Ivanov, S.V., Boldyrev, E.I., et al., *Russ. J. Appl. Chem.,* 2002, vol. 75, no. 9, pp. 1420–1423.
13. Ren, Y., Ma, Z., and Dai, S., *Materials,* 2014, vol. 7, p. 3547.
14. Liang, S.H., Teng, F., Gauge, B.G., et al., *J. Phys. Chem. C,* 2008, vol. 112, p. 5307.
15. Huang, C.-H., Shu, W.-Y., Wu, H.-M., et al., *Tamkang J. Sci. Eng.,* 2008, vol. 11, no. 4, p. 325.
16. Ivanova, N.D., Boldyrev, E.I., Pimenova, K.N., et al., *Russ. J. Appl. Chem.,* 1998, vol. 71, no. 7, pp. 1269–1271.
17. Sinha, A.K., Suzuki, K., Takahara, M., et al., *Angew. Chem., Int. Ed.,* 2007, vol. 46, p. 2891.
18. Zhao, J.C., Wang, J., and Xu, J.L., *J. Chem.,* 2015, vol. 2015, p. 768023. doi doi 10.1155/2015/768023
19. Chen, C.-H. and Suib, L., *J. Chin. Chem. Soc.,* 2012, vol. 59, p. 1.
20. Brock, S.L., Duan, N., Tian, Z.R., et al., *Chem. Mater.,* 1998, vol. 10, p. 2619.
21. Yakovleva, N.M., Yakovlev, A.N., and Chupakhina, E.A., *Thin Solid Films,* 2000, vol. 366, p. 37.
22. Savchenko, O.I., Yakovleva, N.M., Yakovlev, A.N., et al., *Kondens. Sredy Mezhfaznye Granitsy,* 2012, vol. 14, p. 243.
23. Stepanova, K.V., Yakovleva, N.M., Kokatev, A.N., et al., *Uch. Zap. Petrozavodsk. Gos. Univ.,* 2015, vol. 147, no. 2, p. 81.
24. Knorre, G.F., *Topochnye protsessy (Burning Processes)*, Moscow-Leningrad: Gosenergoizdat, 1951.

Translated by D. Marinin